Structural Components of Ryanodine Responsible for Modulation of Sarcoplasmic Reticulum Calcium Channel Function†

William Welch,*,‡ Alan J. Williams,§ Andrew Tinker,§ Kathy E. Mitchell,‡ Pierre Deslongchamps,|| J. Lamothe,|| Koert Gerzon,⊥ Keshore R. Bidasee,⊥ Henry R. Besch, Jr.,⊥ Judith A. Airey,▽ John L. Sutko,▽ and Luc Ruest||

Department of Biochemistry and Department of Pharmacology, University of Nevada, Reno, Nevada 89557, Cardiac Medicine, National Heart and Lung Institute, Imperial College, University of London, Dovehouse Street, London SW3 6LY, United Kingdom, Département de chimie, Université de Sherbrooke, Sherbrooke, Québec J1K2R1, Canada, and Department of Pharmacology and Toxicology, Indiana University School of Medicine, Indianapolis, Indiana 46202-5120

Received September 20, 1996; Revised Manuscript Received December 27, 1996⊗

ABSTRACT: Comparative molecular field analysis (CoMFA) was used to analyze the relationship between the structure of a group of ryanoids and the modulation of the calcium channel function of the ryanodine receptor. The conductance properties of ryanodine receptors purified from sheep heart were measured using the planar, lipid bilayer technique. The magnitude of the ryanoid-induced fractional conductance was strongly correlated to specific structural loci on the ligand. Briefly, electrostatic effects were more prominent than steric effects. The 10-position of the ryanoid had the greatest influence on fractional conductance. Different regions of the ligand have opposing effects on fractional conductance. For example, steric bulk at the 10-position is correlated with decreased fractional conductance, whereas steric bulk at the 2-position (isopropyl position) is correlated with increased fractional conductance. In contrast to fractional conductance, the 3-position (the pyrrole locus) had the greatest influence on ligand binding, whereas the 10-position had comparatively little influence on binding. Two possible models of ryanodine action, a direct (or channel plug) mechanism and an allosteric mechanism, were examined in light of the CoMFA. Taken together, the data do not appear to be consistent with direct interaction between ryanodine and the translocating ion. The data appear to be more consistent with an allosteric mechanism. It is suggested the ryanoids act by inducing or stabilizing a conformational change in the ryanodine receptor that results in the observed alterations in cation conductance.

Ryanodine is a plant alkaloid with powerful pharmacological actions on both skeletal and cardiac muscle. The target of ryanodine is an intracellular calcium release channel known as the ryanodine receptor (RyR).[1] The RyR has been the subject of recent review articles (Meissner, 1994; Coronado *et al*., 1994; Ogawa, 1994; Sutko & Airey, 1996). The RyR mediates calcium release from the sarcoplasmic reticulum (SR) and forms part of the excitation−contraction coupling complex. It is an unusually large protein composed of four identical 565 kDa subunits (Lai *et al*., 1989). Ryanodine receptors have also been detected in a diverse array of other tissues (Shoshan-Barmatz *et al*., 1991; Zaidi *et al*., 1992; Ellisman *et al*., 1990; McPherson & Campbell, 1993; Ledbetter *et al*., 1994; Giannini *et al*., 1992, 1995). The cellular roles served by the RyR in these tissues are not understood. Neuronal RyRs are suggested to function in neurotransmitter release (Padua *et al*., 1996, and references therein).

Ryanodine is a complex modulator of the calcium channel function of the RyR. Ryanodine is thought to bind to the open or conducting form of the RyR calcium channel (Ogawa, 1994; Fleischer & Inui, 1989; McPherson & Campbell, 1993; Meissner & El-Hashem, 1992). At low concentrations of ryanodine, the ligand causes the channel to persist in a partially open (or partially conducting) state (Rousseau *et al*., 1987; Ashley & Williams, 1990). Higher concentrations of ryanodine promote a long-lived, fully closed conformation (Lai *et al*., 1989; Coronado *et al*., 1994; Ogawa, 1994; Tinker *et al*., 1996). It is clear that, although there may be preferential (or even exclusive) binding of ryanodine to the open form of the channel, ryanodine does not act as a simple allosteric modulator or simply stabilize the open conformation of a two-state process. The partially conducting state of the RyR seen at low ryanodine concentrations is not observed in the absence of ryanodine. The closed state observed at high ryanodine concentrations may be the result of a reversion to the closed state observed with the unmodified RyR. Alternatively, the closed state may be the result of the induction of a unique conformation as discussed by Pessah and Zimanyi (1991). Here we focus on the structural properties of ryanoids under conditions that induce the partially conducting state.

Two essential features of the ryanodine receptor remain unknown: (A) the structure of the ryanodine binding site of the RyR and (B) the spatial relationship between the binding

† This work was supported by the American Heart Association (93012790), the National Science Foundation (MCB-9317684), The University of Nevada Molecular Modeling/Graphics Core Facility, the Glaxo Cardiac Discovery Program, The Wellcome Trust, the British Heart Foundation, and the Showalter Trust.

* Corresponding author Phone: 702-784-4102. Fax: 702-784-1419. E-mail: welch@scs.unr.edu.

‡ Department of Biochemistry, University of Nevada.

§ University of London.

|| Université de Sherbrooke.

⊥ Indiana University School of Medicine.

▽ Department of Pharmacology, University of Nevada.

⊗ Abstract published in *Advance ACS Abstracts,* March 1, 1997.

[1] Abbreviations: CoMFA, comparative molecular field analysis; RyR, ryanodine receptor; SR, sarcoplasmic reticulum.

S0006-2960(96)02390-2 CCC: $14.00

Scheme 1

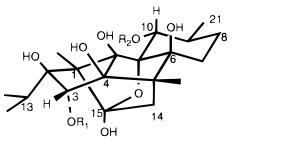

1: Ryanodine: R_1=Pyr; R_2=H
2: Ryanodol: R_1=R_2=H
3: 10-Ryanodine: R_1=H; R_2=Pyr
4: 10-N-CBZ-Glycylryanodine: R_1=Pyr; R_2=CO-$CH_2NHCO_2CH_2C_6H_5$
5: 10-β-Alanylryanodine: R_1= Pyr; R_2=CO-$CH_2CH_2NH_2$
6: 10-O-Guanidinopropionylryanodine: R_1=Pyr; R_2=CO-$CH_2CH_2NHC(NH)NH_2$

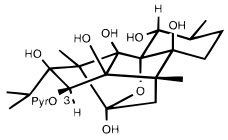

7: 3-Epiryanodine

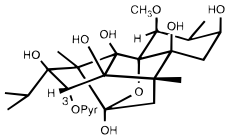

8: Ester A

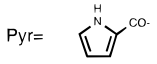

N-CBZ= -NH-CO_2-$CH_2C_6H_5$

Scheme 2

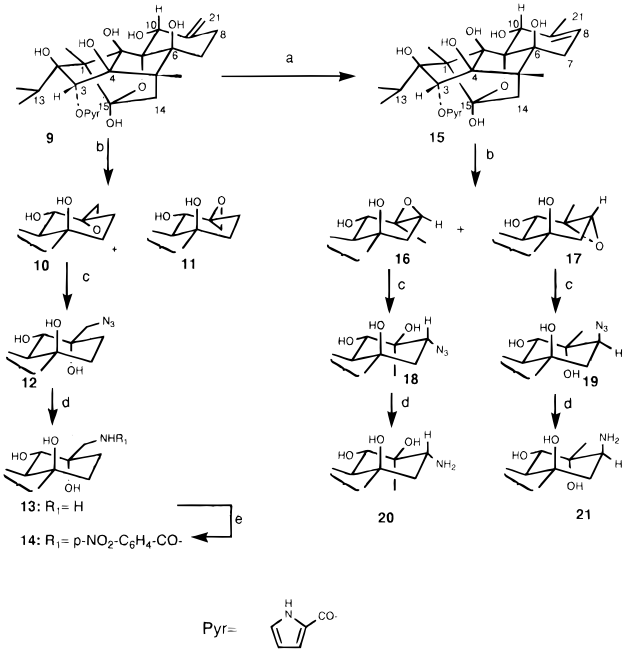

Reaction conditions: a) 10% Pd/C, o-xylene, 120°C, 2h; b) CF_3CO_3H, $NaHCO_3$, $(CH_2Cl)_2$, CH_3CN; c) NaN_3, H_2O, $CH_3OCH_2CH_2OH$; d) H_2, 10%Pd/C, EtOH; e) p-$NO_2C_6H_4COCl$, CH_3CN, Et_3N, 0°C.

site and the ion conduction path. It is unlikely that either will be solved in the near future by crystallographic means. Low-resolution reconstructions of the RyR have been obtained (Wagenknecht & Radermacher, 1995, and references therein). Covalent modification techniques have placed the ryanodine binding site near transmembrane regions in the C-terminal region of the RyR (Callaway *et al*., 1994; Witcher *et al*., 1994). We have applied an alternative strategy. Comparative molecular field analysis (CoMFA; Cramer *et al*., 1988) is a powerful technique capable of producing useful insights into RyR structure and function. We have been employing one aspect of CoMFA to explore the RyR by correlating structural changes in ryanodine analogs to changes in RyR function. Green and Marshall (1995) have reviewed three-dimensional quantitative structure−activity relationship techniques (including CoMFA). They discuss problems in the application of these techniques and outline some of the successes. We have described the structural features correlated with high-affinity binding to skeletal SR (Welch *et al*., 1994). Analysis of structural isomers of ryanodine indicates that the pyrrole locus is the premier structural feature determining orientation of the ligand in the ryanodine binding site (Welch *et al*., 1996). We have proposed a model where the pyrrole group is buried in a binding pocket whereas the 9- and 10-positions are exposed to solvent (Welch *et al*., 1996).

In a related communication, Tinker *et al*. (1996) described the induction of different RyR subconductance states by a series of ryanodine analogs. In this paper, we map the structural features that correlate with the magnitude of the subconductance state. In addition, we extend our earlier observations on the role of the pyrrole in ryanoid binding (Welch *et al*., 1996) and present some of our data on binding of ryanodine analogs to cardiac SR (K. E. Mitchell *et al*., manuscript in preparation).

EXPERIMENTAL PROCEDURES

Synthesis of Ryanoids and Chemical Methods

We describe the synthesis of novel ryanodine analogs used here and in the previous communication (Tinker *et al.*, 1996). First, in Scheme 1, we show some derivatives whose isolation or the syntheses of which have been published elsewhere; besides ryanodine (**1**) (Wiesner, 1972) and ryanodol (**2**) (Wiesner, 1972; Deslongchamps *et al*., 1990), we show 10-(*O*-α-pyrrolylcarbonyl)ryanodol (**3**) (Ruest *et al*., 1993), 10-*N*-CBZ-glycylryanodine (**4**), 10-*β*-alanylryanodine (**5**), 10-(3-guanidinopropionyl)ryanodine (**6**) (Humerickhouse *et al*., 1994), 3-epiryanodine (**7**) (Ruest *et al*., 1993), and ester A (**8**) (Ruest *et al*., 1985; Jefferies *et al*., 1992).

In Scheme 2, we show how, from natural 9,21-didehydroryanodine (**9**), we obtained some new ryanodine derivatives (**10**−**21**) bearing functional groups at positions 8, 9, and 21. Epoxidation of the abundant natural 9,21-didehydroryanodine (**9**) led to a separable mixture of epimeric epoxides **10** and **11**, obtained elsewhere in other conditions (Waterhouse *et al*., 1987). Very recently, the 9α,21-epoxide (**10**) has been observed and isolated as a natural ryanoid from the extracts of *Ryania speciosa* (L. Ruest and M. Dodier, unpublished results). Opening of the oxiran ring of the α-isomer (**10**) by sodium azide yielded azido alcohol **12** which gave 21-amino-9α-hydroxyryanodine (**13**) upon catalytic hydrogenation. This 21-aminoryanodine derivative was converted to its 21-*N*-*p*-nitrobenzoyl derivative (**14**) by classical acylation with *p*-nitrobenzoyl chloride. Alternatively, isomerization of the exocyclic double bond of 9,21-didehydroryanodine (**9**) led to 8,9-didehydroryanodine (**15**) obtained previously in other conditions (Ruest *et al*., 1985). This compound (**15**) was submitted to a reaction sequence identical to the one just described for compound **9** to yield, sequentially, epimeric epoxides **16** and **17** which were opened separately to azido alcohols **18** and **19**. These latter compounds furnished amino alcohols **20** and **21** upon catalytic hydrogenation.

Melting points were determined on a Reichert hot stage apparatus and are uncorrected. Tetrahydrofuran (THF) was distilled from sodium benzophenone ketyl. Dichloromethane, ethylene dichloride, and acetonitrile used for reactions were

distilled over calcium hydride. All reactions were performed under a nitrogen atmosphere. Analytical and preparative thin-layer chromatography were carried out on glass plates precoated with silica gel 60F-250 (Merck). Column chromatography was performed with Merck (200−400 mesh) silica gel. The infrared spectra (IR) were taken on a Perkin-Elmer 681 spectrophotometer. The ^{1}H NMR spectra were recorded on a Bruker Wm-250 instrument (with CHD_2OD as the internal standard centered at 3.30 ppm). The following abbreviations have been used: s, singlet; d, doublet; dd, doublet of doublets; t, triplet; m, multiplet; br, broad. Mass spectra and peak matching (exact mass) were recorded on a VG Micromass ZAB-2F spectrometer.

*9,21α- and 9,21β-Epoxyryanodine (**10**) and (**11**).* A solution of trifluoroperacetic acid (300 μL of a 0.94 M solution in 1,2-dichloroethane, 0.28 mmol) was added to a cold (0 °C), stirred solution of 9,21-didehydroryanodine (**9**) (100 mg, 0.203 mmol) in a mixture of acetonitrile (6 mL) and 1,2-dichloroethane (4 mL) containing solid sodium bicarbonate (200 mg). After 30 min, the mixture was poured into a dilute solution of sodium thiosulfate (0.1 M, 10 mL) and extracted (eight times) with ethyl acetate. The crude mixture (110 mg) was separated on silica plates (9:1 $CHCl_3$/MeOH, three elutions) to yield α-epoxide **10** (50 mg, 48%) and β-epoxide **11** (38 mg, 37%).

*9,21α-Epoxyryanodine (**10**) (less polar):* mp 212−214 °C; ^{1}H NMR (CD_3OD, δ in parts per million throughout) 7.03, 6.88, and 6.24 (three dd for pyrrole ring hydrogens), 5.64 (s, 1H, HC3), 4.38 (s, 1H, HC10), 2.84 (d, J = 5.1 Hz, 1H, H_AC21), 2.58 (d, J = 13.8 Hz, 1H, H_AC14), 2.37 (d, J = 5.1 Hz, 1H, H_BC21), 2.5−2.3 (m, 2H), 2.26 (m, 1H, HC13), 1.96 (d, J = 13.8 Hz, H_BC14), 1.45−1.20 (m, 2H), 1.34 (s, 3H, CH_3C1), 1.10 (d, J = 6.7 Hz, 3H, CH_3C13), 0.92 (s, 3H, CH_3C5), 0.75 (d, J = 6.4 Hz, 3H, CH_3C13); MS (*m*/*e*) 507 (M^+, weak); exact mass calcd for $C_{25}H_{33}O_{10}N$ 507.2104 (M^+), found 507.2097.

*9,21β-Epoxyryanodine (**11**) (more polar):* amorphous solid; ^{1}H NMR (CD_3OD, δ) 7.03, 6.87, and 6.24 (three dd for pyrrole ring hydrogens), 5.644 (s, 1H, HC3), 4.47 (br s, 1H, HC10), 3.17 (br d, J = 5.3 Hz, 1H, H_AC21), 2.58 (d, J = 13.8 Hz, 1H, H_AC14), 2.51 (d, J = 5.3 Hz, 1H, H_BC21), 2.25 (m, 2H), 1.93 (d, J = 13.8 Hz, 1H, H_BC14), 1.5−1.2 (m, 3H), 1.38 (s, 3H, CH_3C1), 1.10 (d, J = 6.6 Hz, 3H, CH_3C13), 0.92 (s, 3H, CH_3C5), 0.75 (d, J = 6.4 Hz, 3H, CH_3C13).

*21-Azido-9α-hydroxyryanodine (**12**).* Sodium azide (103 mg, 1.57 mmol) and water (50 μL) were added to a solution of mixed epoxides **10** and **11** (80 mg, 0.157 mmol, approximately 1:1) in 2-methoxyethanol (2 mL). The mixture was stirred at 80 °C for 2.5 h, cooled, poured into water, and extracted with ethyl acetate (eight times). Column chromatography of the crude product (82 mg, 9:1 $CHCl_3$/MeOH) furnished azido alcohol **12** (22 mg, 25%, ∼50% from pure isomer **10**) and pure 9β,21-epoxyryanodine (**11**) (40 mg, 50%), unchanged under these conditions.

*Azido alcohol **12**:* mp 165−167 °C; IR (ν, $CHCl_3$) 3450 (br), 2210, 1680, 1410, 1220 cm^{-1}; ^{1}H NMR (CD_3OD, δ) 7.03, 6.87, and 6.24 (three dd for pyrrole ring hydrogens), 5.63 (s, 1H, HC3), 4.13 (s, 1H, HC10), 3.38 (d, J = 12 Hz, 1H, H_AC21), 3.34 (d, J = 12 Hz, 1H, H_BC21), 2.59 (d, J = 13.9 Hz, 1H, H_AC14), 2.27 (m, 1H, HC13), 2.3−1.9 (m, 2H), 1.96 (d, J = 13.9 Hz, 1H, H_BC14), 1.68 (m, 1H), 1.40 (s, 3H, CH_3C1), 1.41−1.30 (m, 2H), 1.10 (d, J = 6.7 Hz, 3H, CH_3Cl3), 0.91 (s, 3H, CH_3C5), 0.75 (d, J = 6.4 Hz, 3H, CH_3C13); MS (*m*/*e*): 550 (M^+, absent), 504 ($M^+ - H_2O - N_2$).

*21-Amino-9α-hydroxyryanodine (**13**).* A solution of azido alcohol **12** (34 mg, 0.036 mmol) in dry methanol (2 mL) was transferred to a prehydrogenated mixture of palladium catalyst (10% Pd/C, 5 mg) in dry methanol (4 mL) containing triethylamine (50 μL). The mixture was stirred under hydrogen for 2 h and then filtered, and the solvents were evaporated. The crude product (32 mg) containing a major compound (**13**) was purified by HPLC (CH_3OH/40% H_2O) to give pure amine (30 mg): ^{1}H NMR (CD_3OD, δ) 7.04, 6.87, and 6.24 (three dd for pyrrole ring hydrogens), 5.63 (s, 1H, HC3), 4.19 (s, 1H, HC10), 5.63 (s, 1H, HC3), 4.19 (s, 1H, HC10), 2.89 (d, J = 13.1Hz, 1H, H_AC21), 2.68 (d, J = 13.1Hz, 1H, H_BC21), 2.60 (d, J = 13.9 Hz, 1H, H_AC14), 2.22 (m, 2H, HC13, $H_{ax}C7$), 1.98 (d, J = 13.9 Hz, 1H, H_BC14), 1.88, 1.62, and 1.35 (three m for $H_{ax}C8$, $H_{eq}C7$, and $H_{eq}C8$), 1.41 (s, 3H, CH_3C1), 1.10 (d, J = 6.7 Hz, 3H, CH_3C13), 0.92 (s, 3H, CH_3C5), 0.75 (d, J = 6.4 Hz, 3H, CH_3C13); MS (*m*/*e*) 524 (M^+, weak); exact mass calcd for $C_{25}H_{33}O_{10}N$ ($M^+ - NH_3$) 507.2104, found 507.2112.

*21-Amino-21-N-(p-nitrobenzoyl)-9α-hydroxyryanodine (**14**).* *p*-Nitrobenzoyl chloride (3 mg, 0.043 mmol) was added to a cold (0 °C) solution of crude amino alcohol **13** (20 mg, 0.038 mmol) in acetonitrile (0.2 mL) and triethylamine (0.1 mL). The mixture was stirred for 30 min, treated with methanol (120 μL), and poured into dilute sodium bicarbonate solution and extracted with ethyl acetate (five times). The crude product was purified on a silica plate (94:6 $CHCl_3$/MeOH, two elutions), to yield benzamide derivative **14** (6 mg, 58%): ^{1}H NMR (CD_3OD, δ) 8.31 (d, J = 8.9 Hz, 2H, benzoate ortho hydrogens), 8.03 (d, J = 8.9 Hz, 2H, benzoate meta hydrogens), 7.03, 6.87, and 6.23 (three dd for pyrrole ring hydrogens), 5.63 (s, 1H, HC3), 4.20 (s, 1H, HC10), 3.68 (s, J = 13.5 Hz, 1H, H_AC21), 3.43 (d, J = 13.5 Hz, 1H, H_BC21), 2.60 (d, J = 13.9 Hz, 1H, H_AC14), 2.25 (m, HC13), 2.3−1.9 (m, 2H), 1.98 (d, J = 13.8 Hz, 1H, H_BC14), 1.67 (m, 1H), 1.43 (s, 3H, CH_3C1), 1.35 (m, 1H), 1.10 (d, J = 6.8 Hz, 2H, CH_3C13), 0.91 (s, 3H, CH_3C5), 0.75 (d, J = 6.4 Hz, 3H, CH_3C13); MS (*m*/*e*) 639 ($M^+ - 2H_2O$).

*8,9-Didehydroryanodine (**15**).* A suspension of palladium catalyst (40 mg, 10% Pd/C) in dry *o*-xylene (6 mL) was stirred under hydrogen for 10 min and then desorbed (under partial vacuum), and the hydrogen atmosphere was replaced by nitrogen. To this activated catalyst suspension was added a solution of 9,21-didehydroryanodine (**9**) (70 mg, 0.142 mmol) in THF. The mixture was heated at 120 °C (removal of low-boiling THF) for 2 h. The cooled mixture was then filtered, and the solvent was evaporated to yield known (Ruest *et al*., 1985) olefin **15** (70 mg, 99%): mp 183−185 °C.

*8β,9- and 8α,9-Epoxyryanodine (**16** and **17**).* A solution of trifluoroperacetic acid (0.94 M in 1,2-dichloroethane, 130 μL, 0.122 mmol) was added to a cold (0 °C) solution of 8,9-didehydroryanodine (**15**) (52 mg, 0.106 mmol) in 1,2-dichloroethane (4 mL) and acetonitrile (4 mL) containing solid sodium bicarbonate (120 mg). After 1 h, the mixture was poured into a solution of sodium thiosulfate (0.1 M, 10 mL) and extracted with ethyl acetate. Chromatography (9:1 $CHCl_3$/CH_3OH) of the crude product afforded 8β,9-epoxide **16** (9 mg, 18%, less polar) and 8α,9-epoxide **17** (32 mg, 63%).

*8β,9-Epoxyryanodine (**16**):* amorphous solid; ^{1}H NMR (CD_3OD, δ) 7.02, 6.85, and 6.23 (three dd for pyrrole ring hydrogens), 5.63 (s, 1H, HC3), 4.14 (br s, 1H, HC10), 3.31 (m, 1H, H_αC8), 2.64 (d, J = 14.0 Hz, 1H, H_AC14), 2.47 (dd, J = 15.1 and 2.0 Hz, 1H, HC7), 2.23 (qn, J = 6.5 Hz, 1H, HC13), 1.94 (d, J = 14.0 Hz, 1H, H_BC14), 1.84 (dd, J = 15.1 and 1.8 Hz, 1H, HC7), 1.40 (br s, 3H, CH_3C9), 1.39 (s, 3H, CH_3C1), 1.09 (d, J = 6.7 Hz, 3H, CH_3C13), 0.90 (s, 3H, CH_3C5), 0.73 (d, J = 6.4 Hz, 3H, CH_3C13).

*8α,9-Epoxyryanodine (**17**):* mp 204−208 °C; ^{1}H NMR (CD_3OD, δ) 7.03, 6.87, and 6.23 (three dd for pyrrole ring hydrogens), 5.60 (s, 1H, HC3), 4.18 (s, 1H, HC10), 3.13 (d, J = 5.8 Hz, 1H, H_βC8), 2.57 (d, J = 13.9 Hz, 1H, H_AC14), 2.34 (d, J = 14.7 Hz, 1H, H_αC7), 2.23 (qn, J = 6.6 Hz, 1H, HC13), 1.86 (d, J = 13.9 Hz, 1H, H_BC14), 1.71 (dd, J = 14.7 and 5.8 Hz, 1H, H_βC7), 1.41 (s, 3H, CH_3C1), 1.33 (s, 3H, CH_3C9), 1.08 (d, J = 6.7 Hz, 3H, CH_3C13), 0.87 (s, 3H, CH_3C5), 0.74 (d, J = 6.4 Hz, 3H, CH_3C13); MS (*m*/*e*) 507 (M^+); exact mass calcd for $C_{25}H_{33}O_{10}N$ 507.2104 (M^+), found 507.2097.

*8α-Azido-9β-hydroxyryanodine (**18**).* A mixture of minor β-epoxide **16** (8 mg, 0.015 mmol), sodium azide (10 mg), and water (15 μL) in 2-methoxyethanol (0.5 mL) was heated (85 °C) for 1.5 h, then cooled, and filtered, and the solvent was evaporated. Purification by silica plate chromatography (85:15 $CHCl_3/CH_3OH$) afforded azido alcohol **18** (5 mg, 60%); mp 172−175 °C; IR (ν, $CHCl_3$) 2220 cm^{-1}; ^{1}H NMR (CD_3OD, δ) 7.03, 6.87, and 6.23 (three dd for pyrrole ring hydrogens), 5.61 (s, 1H, HC3), 4.23 (s, 1H, HC10), 3.97 (dd, J = 12.2 and 5.0 Hz, 1H, H_{ax}C8), 2.56 (d, J = 13.5 Hz, 1H, H_AC14), 2.24 (qn, J = 6.5 Hz, HC13), 2.04 (dd, app t, J = 12.3 Hz, H_{ax}C7), 1.84 (d, J = 13.7 Hz, 1H, H_BC14), 1.59 (dd, J = 12.3 and 5.0 Hz, 1H, H_{eq}C7), 1.39 (s, 3H, CH_3C1), 1.33 (s, 3H, CH_3C9), 1.09 (d, J = 6.7 Hz, 3H, CH_3C13), 0.91 (s, 3H, CH_3C5), 0.74 (d, J = 6.4 Hz, 1H, CH_3C13); MS (*m*/*e*) 504 ($M^+ - N_2 - H_2O$).

*8β-Azido-9α-hydroxyryanodine (**19**).* A mixture of α-epoxide **17** (20 mg, 0.039 mmol), sodium azide (45 mg), and water (20 μL) in 2-methoxyethanol was heated (95 °C) for 2 h, then cooled, and filtered, and the solvent was evaporated. The residue was chromatographed on a silica plate [9:1:0.1 $CHCl_3/CH_3OH$ (40%)/$CH_3NH_2 \cdot H_2O$] to yield 8β-azido-9α-hydroxyryanodine (**19**) (12 mg, 55%); mp 185−190 °C; IR (ν, $CHCl_3$) 3450 (br), 2220 cm^{-1}; ^{1}H NMR (CD_3OD, δ) 7.03, 6.86, and 6.24 (three dd for pyrrole ring hydrogens), 5.63 (s, 1H, HC3), 4.11 (s, 1H, HC10), 3.79 (dd, J = 4.9 and 1.9 Hz, 1H, H_{eq}C8), 2.64 (d, J = 14.1 Hz, 1H, H_AC14), 2.53 (dd, J = 14.7 and 4.9 Hz, 1H, H_{ax}C7), 2.22 (qn, J = 6.6 Hz, 1H, HC13), 1.93 (d, J = 14.1 Hz, 1H, H_BC14), 1.70 (dd, J = 14.7 and 1.9 Hz, 1H, H_{eq}C7), 1.41 (s, 3H, CH_3C1), 1.35 (s, 3H, CH_3C9), 1.09 (d, J = 6.7 Hz, 3H, CH_3C13), 0.95 (s, 3H, CH_3C5), 0.74 (d, J = 6.4 Hz, 3H, CH_3C13); MS (*m*/*e*) 550 (M^+, weak), 504 ($M^+ - N_2 - H_2O$).

*8α-Amino-9β-hydroxyryanodine (**20**).* A solution of azide **18** (2 mg, 0.0036 mmol) in ethanol (0.5 mL) was transferred to a prehydrogenated mixture of palladium catalyst (10% Pd/C, 5 mg) in ethanol (1 mL) containing triethylamine (25 μL). The mixture was stirred under hydrogen for 1.5 h and then filtered, and the solvent was evaporated. Chromatography on silica plates [75:25:1.5 $CHCl_3/CH_3OH$ (40%)/$CH_3NH_2 \cdot H_2O$] gave amino derivative **20** (1.7 mg, ∼80%): ^{1}H NMR (CD_3OD, δ) 7.04, 6.88, and 6.24 (three dd for pyrrole ring hydrogens), 5.61 (s, 1H, HC3), 4.25 (s, 1H, HC10), 3.45 (dd, J = 14 and 4 Hz, 1H, H_{ax}C8), 2.59 (d, J = 13.8 Hz, 1H, H_aC14), 2.26 (qn, J = ∼ 6 Hz, 1H, HC13), 2.05 (dd, app t, J = ∼ 14 Hz, 1H, H_{ax}C7), 1.84 (d, J = 13.7 Hz, 1H, H_BC14), 1.73 (dd, J = ∼ 14 and 4 Hz, 1H, H_{eq}C7), 1.41 (s, 3H, CH_3C1), 1.34 (s, 3H, CH_3C9), 1.10 (d, J = 6.8Hz, 3H, CH_3C13), 0.94 (s, 3H, CH_3C5), 0.75 (d, J = 6.4 Hz, 3H, CH_3C13); MS (*m*/*e*) 524 (M^+).

*8β-Amino-9α-hydroxyryanodine (**21**).* The procedure just described for reduction of azide **20** was applied to azide **19** (7 mg, 0.013 mmol). The crude reaction product was purified on silica plate [90:10:1.5 $CHCl_3/CH_3OH$ (40%)/$CH_3NH_2 \cdot H_2O$] to give amine **21** (5 mg, 75%): mp 235−240 °C dec; ^{1}H NMR (CD_3OD, δ) 7.04, 6.88, and 6.25 (three dd for pyrrole ring hydrogens), 5.62 (s, 1H, HC3), 4.23 (s, 1H, HC10), 3.37 (br d, J = ∼ 4 Hz, 1H, H_{eq}C8), 2.61 (d, J = 14.1 Hz, 1H, H_AC14), 2.51 (dd, J = ∼ 14 and 4 Hz, 1H, H_{ax}C7), 2.24 (qn, J = 6.6 Hz, 1H, HC13), 1.93 (d, J = 14.1 Hz, 1H, H_BC14), 1.60 (dd, J = 13.8 and 1.7 Hz, 1H, H_{eq}-C7), 1.42 (s, 3H, CH_3C1), 1.366 (s, 3H, CH_3C9), 1.10 (d, J = 6.7 Hz, 3H, CH_3C13), 0.96 (s, 3H, CH_3C5), 0.75 (d, J = 6.4 Hz, 3H, CH_3C13); MS (*m*/*e*) 524 (M^+); exact mass calcd for $C_{25}H_{36}O_{10}N_2$ 524.2370, found 524.2380.

Abbreviations Used

The following abbreviations are used to be consistent with a previous communication (Tinker *et al*., 1996). Ester A ryanodine (**8**) is referred to as ester A, CBZ-glycylryanodine (**4**) as CBZ glycyl, 21-[(*p*-nitrobenzoyl)amino]-9-hydroxyryanodine (**14**) as 21-*p*-nitro, β-alanylryanodine (**5**) as β-alanyl, (guanidinopropionyl)ryanodine (**6**) as guanidinopropionyl, 9,21-dehydroryanodine (**9**) as 9,21 dehydro, 9β,-21β-epoxyryanodine (**11**) as epoxyryanodine, 9-hydroxy-21-azidoryanodine (**12**) as azidoryanodine, 10-pyrrolylryanodol (**3**) as 10-pyrrole (also called 10-ryanodine), and 3-epiryanodine (**7**) as 3-epi.

Preparation of SR Membranes for Binding Measurements

Rabbit cardiac SR membranes were prepared in a manner similar to that previously described (Airey *et al*., 1990; Campbell *et al*., 1980; Humerickhouse *et al*., 1993; Meissner, 1975; Welch *et al*., 1994). Briefly, hearts were dissected, frozen in liquid nitrogen, and stored at −80 °C. The frozen tissue was homogenized and the heavy sarcoplasmic reticulum fraction isolated by differential centrifugation. This preparation was aliquoted, frozen with liquid nitrogen, and stored at −80 °C. The consistency of the SR preparations was monitored. A randomly selected aliquot of each preparation was thawed, and the ryanodine binding was measured using the direct assay described previously (Welch *et al*., 1996). The affinity for ryanodine (see Table 1) and the total number of high-affinity binding sites (1 pmol/mg) are similar to that reported by others. For example, Zucchi *et al*. (1995) obtained 1.3 nM and 2.2 pmol/mg, respectively.

Measurement of Channel Conductance

The modulation of calcium channel conductance was determined using the planar lipid bilayer technique (Tinker *et al*., 1996) using the RyR prepared from sheep hearts as described in that paper. Briefly, the RyR was solubilzed from SR isolated by desity gradient centrifugation. Potassium ion was the charge carrier. The measured values,

Table 1: Dissociation Constants of Ryanoid Binding and Induced Fractional Conductance[a]

ryanoid	dissociation constant (nM)	fractional conductance (%)		
		experimental	total[b]	steric[b]
ryanodine	2.1	56.8	58	57
9,21 dehydro	2.1	58.3	58	57
ryanodol	1630	69.4	68	66
ester A	5	61.5	57	53
epoxyryanodine	30	56.8	59	56
azidoryanodine	25	56.3	55	55
10-pyrrole	13	52.2	54	57
3-epi	178	42.9	43	48
CBZ glycyl	17	29.4	26	31
21−*p*-nitro	19	26.1	29	33
β-alanyl	0.61	14.3	11	50
guanidinopropionyl	0.55	5.8	8	48

[a] The binding data were obtained from measurements performed on rabbit cardiac muscle at Reno. The fractional conductance was measured in London [see Tinker *et al*. (1996) for further details]. [b] The total column contains the predicted values of the fractional conductance derived from the CoMFA analysis. The steric column contains the predicted values, ignoring all of the electrostatic components of the CoMFA. The same CoMFA model was used for both calculations. Molecules in identical conformation and orientation were used. The only difference was that the charges on the molecules were set to zero.

reported as fractional conductance, are summarized in Table 1 for ease of reference by the reader.

Comparative Molecular Field Analysis (CoMFA)

The conformational minima of the molecules were determined as described previously (Welch *et al*., 1994) using the SYBYL package and the Tripos force field (Clark *et al*., 1989). The molecules were then aligned to ryanodine using a rigid-body, field-fit algorithm. The relationship between the structure and the magnitude of the subconductance state was analyzed using CoMFA (Cramer *et al*., 1988). Unless otherwise stated, all analyses were conducted with the minimum $\Sigma = 0$ and a 1 Å grid. Both electrostatic and steric fields were calculated. The partial least-squares statistical technique was used to find correlations between physical and biological properties. A cross-validated r^2 of 0.3 or greater (the maximum value is 1) is considered to be indicative of a model with useful predictive ability (less than 5% probability that the correlation is due to chance) [SYBYL instruction manual, and see Cho and Tropsha (1995)].

RESULTS

Our previous structure−function analyses have focused on the factors responsible for the high-affinity binding of ryanodine to the RyR. In this paper, we have focused on another biological property, modulation of the channel properties of the RyR. In this investigation, we have taken advantage of the synthetic bilayer technique and measured the channel properties of a single RyR. An example of such an experiment is shown in Figure 1. When the channel opens, there is an increase in the current flow across the artificial bilayer (a downward fluctuation in the tracing). Note that the channel rapidly fluctuates between the open and closed state as the time of observation increases from left to right. When ryanodol binds to the RyR (at the arrow), the channel conductance fails to reach the levels of the unmodified RyR. The ratio of the conductance of the modified to

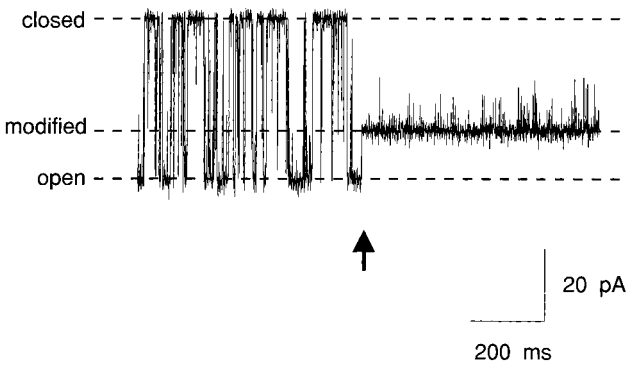

FIGURE 1: Modification of channel function by ryanodol. The figure shows current fluctuations of a purified sheep cardiac ryanodine receptor channel incorporated into a planar phospholipid bilayer at a holding potential of 60 mV with 210 mM K^+ (200 mM KCl and 20 mM HEPES titrated to pH 7.4 with KOH) as the permeant ion on both sides of the membrane. The data were low-pass filtered at 1 kHz with an eight-pole Bessel filter and digitized at 4 kHz using Satori (Intracel, Cambridge, U.K.). For more details of the experiments and the methods used, see Tinker *et al*. (1996). In the experiment illustrated, 20 μM ryanodol is present in the solution at the cytosolic face of the channel. Under these conditions, we observe spontaneous transitions between open and closed states of the channel. The interaction of ryanodol with the channel (indicated by the arrow) results in a dramatic alteration in both channel gating and conductance; the channel enters a long-lived open state with conductance intermediate between the normal open and closed levels. The conductance of this modified state differs for each derivative examined in this study. We have quantified the modification of conductance induced by the ryanoids as fractional conductance (the ratio of the chord conductance at 60 mV before and after modification; Tinker *et al*., 1996).

unmodified RyR is expressed as the fractional conductance. Modification also prevents the rapid opening and closing of the channel. All ryanoids we have thus far tested cause the ryanodine receptor to enter a long-lived, partially conducting open state (Tinker *et al*., 1996). The magnitude of the fractional conductance varied with the structure of the ryanoid (Table 1).

CoMFA of Fractional Conductance

Initial Alignment. The goal of this work was to identify regions of ryanoid structure correlated with the magnitude of the ligand-induced subconductance state. An initial basis set was constructed by eliminating 3-epi and 10-pyrrole from the set of the compounds listed in Table 1. This initial set was chosen because there is little ambiguity about how the members of this group of ryanoids should be aligned with respect to each other. Because of the large structural isomerism, the mutual orientation of ryanodine, 3-epi, and 10-pyrrole in the RyR binding site is a complex issue (Welch *et al*., 1996). All of the molecules in the initial basis set were rigid-body field-fit to ryanodine using the algorithm that is part of the SYBYL/CoMFA package. Very strong correlations were found between fractional conductance and structure with a cross-validated r^2 of 0.758 (two components) and a final r^2 of 0.976. Therefore, the CoMFA of the initial basis set yielded a useful model correlating structure to the induced fractional conductance.

Final Alignment. Next, the initial basis set was employed to predict the fractional conductance of the two omitted members of the set, 3-epi and 10-pyrrole. The objective of this step was to find the alignments of the latter ryanoids yielding predicted values closest to the experimentally

measured values of fractional conductance. Predictions from the initial model have an estimated error of ±4%. The experimentally measured fractional conductance of 3-epi was 42.9 ± 0.7%. The principal alignment schemes tested were as follows: (A) 3-Epi aligned with ryanodine by the pyrrole atoms yielded a predicted fractional conductance of 48.5%. (B) Field fitting of alignment A to ryanodine yielded a predicted fractional conductance of 45% (this was the best alignment). (C) 3-Epi aligned to ryanodine by positions 1−4 (this alignment assumes that 3-epi and ryanodine bind to the RyR in the same orientation) yielded a predicted value of 61%. (D) Field fitting of alignment C yielded a predicted fractional conductance of 57%. Alignments A and B are in agreement with those deduced from the CoMFA of binding data (Welch *et al*., 1996).

The initial CoMFA model was also used to predict the effect of 10-pyrrole (experimental value = 52%). Using the same alignment algorithm described in the paragraph above, the results are as follows: (alignment A) 50%, (alignment B) 53%, (alignment C) 64%, and (alignment D) 62%. For both 3-epi and 10-pyrrole, the alignments have important implications for molecular recognition by the RyR. Alignments A and B imply that the pyrrole binds to the same subsite on the RyR whereas the polycyclic ring system can be accommodated in a variety of orientations. Alignments C and D imply that the polycyclic ring system of ryanodine isomers bind to the RyR in the same orientation whereas the pyrrole can be accommodated in a variety or orientations. Previously, we had shown that the most likely binding mode of these two ryanodine isomers was with the pyrrole locus occupying the same position in the binding site as the pyrrole group of ryanodine (Welch *et al*., 1996). The data indicate clearly that predicted values of fractional conductance are consistent with the hypothesis that the pyrrole group is a major factor determining the alignment of a ryanoid in the RyR binding site.

Using the alignment information described in the preceding paragraphs, a second basis set containing all compounds listed in Table 1 was constructed. Alignments of the ryanodine isomers identified above as giving the best agreement between predicted and experimental fractional conductance were field-fit to ryanodine. The cross-validated r^2 fell slightly from 0.758 to 0.735 (minimum $\Sigma = 0$, optimum number of components = 2). The final r^2 was 0.958 with a standard error in the fractional conductance of ±5%.

In a CoMFA analysis (Cramer *et al*., 1988), a three-dimensional grid is constructed around the set of molecules. For each molecule in the set, the corresponding steric (Lennard-Jones potential) and electrostatic (Coulombic) energy is calculated at each grid point. The changes in these values are correlated to changes in the biological properties. Some results are reported in the preceding paragraphs. Of the total correlation between structure and activity, the fractional contribution of the steric component was 0.41 and the electrostatic contribution was 0.59 (in other words, changes in electrostatic field are more strongly correlated to changes in fractional conductance than changes in steric field). This suggests that changes in fractional conductance are somewhat more sensitive to changes in charge than in molecular shape.

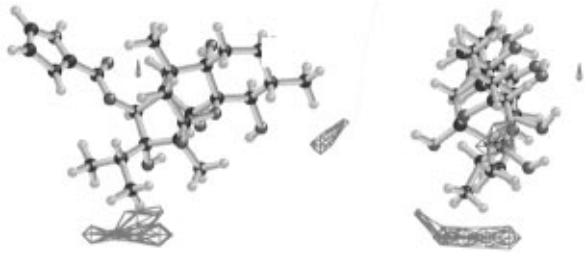

FIGURE 2: Steric factors associated with high channel conductance. The wire frame shows those regions of the molecule where increasing steric bulk is strongly correlated with high values of fractional conductance. Both regions are below the plane of the left illustration. A ball and stick representation of ryanodine is shown to orient the viewer. Orthogonal views are presented in Figures 2−9. The left view is looking toward the hydrophobic side with the pyrrole ring (at the 3-position) to the upper left. The right view is looking toward the 9-position with the hydrophilic side on the right. The wire frames in the figures connect the points in a 1 Å three-dimensional grid having the same value. Therefore, the wire frame describes a constant-value surface. In Figures 2−5, the wire frame contours points of equal strength of the correlation of a particular physical property to a biological property. The correlation is calculated as the product of the standard deviation at each grid point times the coefficients obtained from partial least squares. The points within the volume enclosed by the wire frame are more strongly correlated with the biological property than those on the surface.

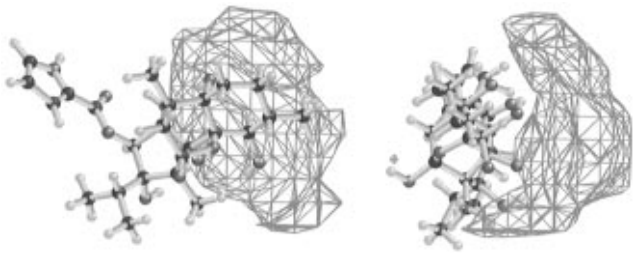

FIGURE 3: Steric factors associated with low fractional conductance. The wire frame shows those regions of the molecule where increasing steric bulk strongly correlates with lower values of fractional conductance. The wire frame is below the plane of the illustration. The contour level is twice that used in Figure 2. A ball and stick representation of ryanodine is shown to orient the viewer.

Correlation of Structure and Fractional Conductance

The percent fractional conductance of the RyR channel can vary from 0 (fully closed) to 100% (fully open). Although the experimentally observed range was wide (6−69%), none of the ryanoids tested induced either extreme. What modifications to the basic ryanodine structure are correlated to changes in fractional conductance? The relationship is illustrated in Figures 2−5. In this data set, the decreases in fractional conductance (relative to ryanodine) were larger in magnitude than the increases. Nonetheless, significant correlations between structure and fractional conductance were found in both cases (*e.g.* Figures 2 and 3).

Steric Effects. Figures 2 and 3 depict the regions of the molecule where steric bulk is correlated with increases (Figure 2) and decreases (Figure 3) in fractional conductance. Figure 3 is contoured at about twice the level used in Figure 2. The presence of steric bulk in the bay formed by the 9-, 10-, and 21-positions, at the isopropyl group (2-position), and at the 4-position is most strongly correlated with high fractional conductance (Figure 2). This trend is opposed by a large area where increasing steric bulk is correlated to decreasing fractional conductance (Figure 3). The area

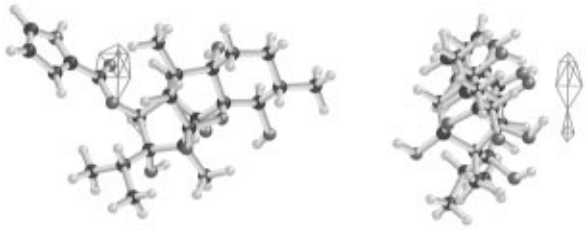

FIGURE 4: Electrostatic factors associated with high fractional conductance. The wire frame shows the region where increasing positive charge is most strongly correlated with higher values of fractional conductance. The wire frame is below the plane of the molecule. The contour level is 3 times that used in Figure 2. A ball and stick representation of ryanodine is shown to orient the viewer.

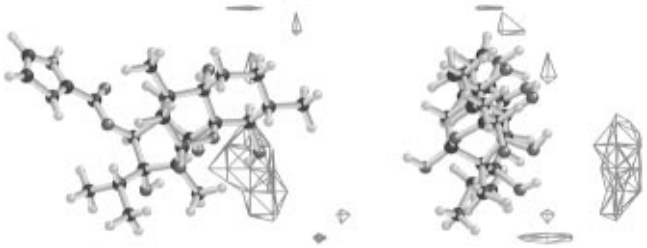

FIGURE 5: Electrostatic factors associated with low fractional conductance. The wire frame shows the regions where increasing positive charge is most strongly correlated with lower values of fractional conductance. The contour level is 3 times that used in Figure 2. A ball and stick representation of ryanodine is shown to orient the viewer.

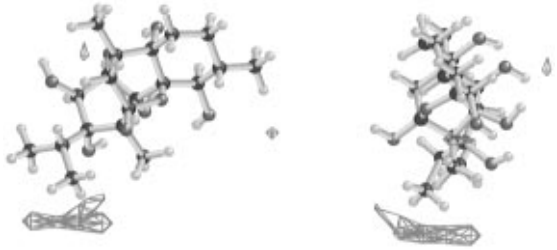

FIGURE 6: Explanation of the steric contribution of ryanodol to fractional conductance. Ryanodol is shown with wire frames contoured to illustrate those parts of the ryanodol structure where the steric bulk of the molecule is estimated to contribute most strongly to the large fractional conductance. The wire frame connects points with equal values. The values in Figures 6−9 are obtained by multiplying the coefficients of the CoMFA by the field strength (in kilocalories per mole).

occupies one face of the ring formed by positions 6−11 and includes the 21-position. The strong steric correlations with decreased fractional conductance lie on the hydrophilic face of ryanodine [see Welch *et al*. (1994)]. The effect of steric bulk at the 10-position is readily seen; all of the ryanoids with bulky substituents at the 10-position have lower fractional conductances than ryanodine, the parent compound. The 10-(pyrrolylcarbonyl) ryanodine (10-pyrrole) is a special case. As described above, the pyrrole at the 10-position assumes the same orientation in the binding site as the pyrrole in ryanodine.

Electrostatic Effects. The relationship between electrostatic potential and fractional conductance is also localized to discrete regions of the ryanoid molecule. Increases in positive potential in the region of position 3 are strongly correlated with increases in fractional conductance (Figure 4). This area extends out to the carbonyl oxygen of the pyrrolylcarbonyl group. In contrast, increases in positive

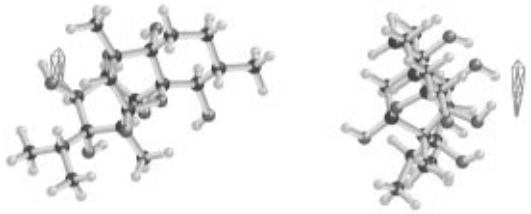

FIGURE 7: Explanation of the electrostatic contribution of ryanodol to fractional conductance. Ryanodol is shown with wire frames contoured at 1.55 times the value in Figure 6 to illustrate the region where the positive electrostatic field is estimated to contribute most strongly to the large fractional conductance. The larger contour value is the result of the stronger correlation between electrostatic factors and fractional conductance compared to the correlation with steric factors (see text).

potential in the regions of the 8- and 10-positions are equally strongly correlated with decreases in fractional conductance (Figure 5). It is striking that the preponderance of electrostatic and steric correlations with channel conductance lies on the same molecular hemisphere.

Although the interrelationships between the steric and Coulombic factors are subtle, the effect of increasing positive charge can be appreciated qualitatively by comparing CBZ glycyl and guanidinopropionyl. Both compounds bear bulky groups at the 10-position; the positive charge on the guanidino derivative results in a much smaller percent fractional conductance (Table 1).

Illustration of How Structure Alters Fractional Conductance

Two extreme examples, ryanodol and guanidinopropionyl, will be used to illustrate the relationship between structure and channel conductance. Of the group of ryanoids tested, ryanodol produces the largest fractional conductance in the channel and has the smallest molecular volume. In the section above, the general trends in the entire data set were visualized by plotting correlations between changes in structure and changes in fractional conductance. It is also of interest to know the location and relative strength of the properties of a particular molecule, such as ryanodol, that explain the biological properties. One approach is to multiply the molecular field surrounding the molecule by the coefficients obtained from the partial least-squares analysis. The results of such a calculation are shown in Figures 6−9. Because the correlation between changes in the electrostatic field and fractional conductance is higher than changes in the steric field (see Results) and because the magnitude of the two fields are different, the results of the product of coefficient times field (Figures 6−9) were normalized. This was accomplished by contouring the steric and electrostatic fields at $^1/_3$ of the maximum values of the respective fields seen in guanidinopropionyl. As a result, the contour level of the electrostatic field is 1.55 times that of the steric field (that is, the absolute values of the grid points in the electrostatic maps are 1.55 times greater than the corresponding points in the steric maps).

The regions where the steric bulk of ryanodol most strongly contributes to the observed fractional conductance are illustrated in Figure 6. The isopropyl group at the 2-position is an important factor in the large fractional conductance induced by this compound. A smaller contribution is localized in the bay formed by the 9-, 10-, and 21-

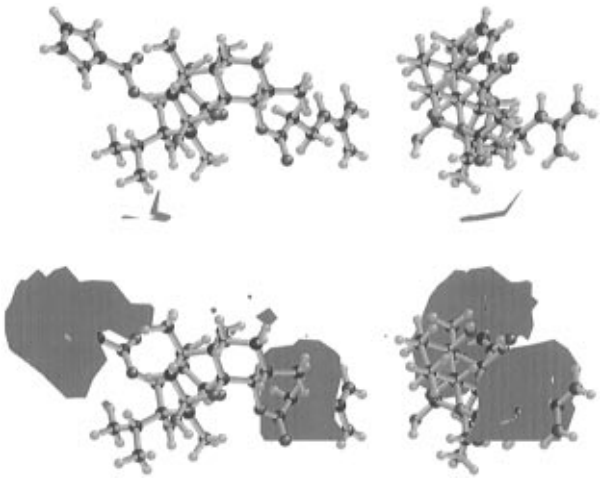

FIGURE 8: Explanation of the steric contribution of guanidinopropionyl to fractional conductance. Guanidinopropionyl is shown with surfaces contoured at the same level as that in Figure 6 to illustrate the major regions where the steric bulk is estimated to contribute to large (upper pair) and small (lower pair) fractional conductance. The opaque surface has the same meaning as the wire frames.

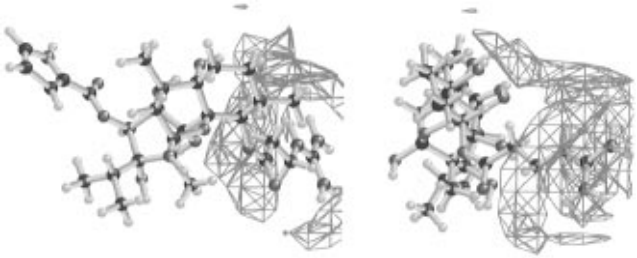

FIGURE 9: Explanation of the electrostatic contribution of guanidinopropionyl to fractional conductance. Guanidinopropionyl is shown with a wire frame contoured at the same level as that of Figure 7 to illustrate the positive electrostatic field of the molecule estimated to contribute most strongly to the low fractional conductance.

positions. Steric factors responsible for lowering fractional conductance are relatively minor (less than $^1/_3$ of the maximum seen in guanidino-propionyl) and are not illustrated. The positive electrostatic field in the region of the 3-position contributes most of the electrostatic component of the relatively high fractional conductance of ryanodol (Figure 7). The other electrostatic properties of ryanodol leading to decreased fractional conductance are relatively weak and are not illustrated. Therefore, steric and electrostatic factors act in concert to produce the observed large fractional conductance of ryanodol.

In contrast to ryanodol, the guanidinium derivative of ryanodine produces the smallest channel fractional conductance and has one of the larger molecular volumes of the ryanoids examined here. When the properties are visualized (Figures 8 and 9) in the same manner as above, the ability of the guanidinopropionyl molecule to lower channel conductance is readily understood. The interplay between structural factors favoring large and small fractional conductances can be appreciated by comparing the upper and lower pairs in Figure 8. As is the case for ryanodol, the steric bulk in the region of the isopropyl group is the primary element favoring high fractional conductance. In contrast, steric factors at the guanidinium group at the 10-position and the pyrrole at the 3-position are major contributors to the low fractional conductance of this compound (Figure 8, lower pair) and overwhelm the factors favoring large fractional conductances. The large positive electrostatic field of the guanidinium group at the 10-position causes the channel to be a poor conductor of cations (Figure 9). In contrast to the positive electrostatic field, the negative electrostatic field appears to have only weak effects on fractional conductance. It is below the contour level used in these illustrations and is not shown.

In summary, the major structural features of the tested ryanodine analogs that modulate fractional conductance are as follows: Steric bulk at the isopropyl group and positive charge at the 3-position favor a larger fractional conductance. In opposition, steric bulk at the pyrrole and 10-positions and positive charge at the 10-position favor a small fractional conductance.

DISCUSSION

Correlation between Ryanoid Structure and Fractional Conductance

Importance of the Pyrrole Group. Previously, we advanced the thesis that the pyrrole carbonyl group is a dominant factor in ryanoid binding (Welch *et al*., 1996). Using a CoMFA of high-affinity ryanoid binding, we presented evidence that the pyrrole carbonyl group guided the orientation of structural isomers of ryanodine in the high-affinity binding site on the RyR. All of the isomers were oriented so that the pyrrole group could occupy the pyrrole subsite in the ryanodine binding site on the RyR. In this paper, we report an analysis of the relationship between structure and a different measure of biological activity, fractional conductance. The analysis fully supports the earlier conclusion. In other words, the CoMFA for the fractional conductance predicts the same orientation of ligand in the binding site as that predicted by the CoMFA of the binding data.

Opposing Effects on Fractional Conductance. The CoMFA of fractional conductance revealed an unexpected insight into ryanoid interaction with the RyR. Although all of the ryanoids tested reduced fractional conductance, the CoMFA of fractional conductance revealed two opposing steric effects. First, the presence of steric bulk at three loci (the 2-position, the 4-position, and the bay at the 9-, 10-, and 21-positions) is correlated with high fractional conductance (Figure 2). Second, increased steric bulk on the hydrophilic face of the fused ring system (formed by positions 7−11) is correlated with decreased fractional conductance (Figure 3). The first effect is weaker than the second. Regional opposition is also observed for electrostatic charge. Increasing positive charge near the 3-position is correlated with increased fractional conductance. In contrast, increasing positive charge at the opposite end of the molecule (the 10-position) is correlated with decreased fractional conductance. On the basis of the present basis set, negative charge appears to have little correlation with fractional conductance. When the analysis was applied to specific compounds (Figures 6−9), the general trends were observed together with locations reflecting the specific characteristics of the interaction of each ryanoid with the RyR.

General Model of the Ryanodine Binding Site. What does binding affinity tell one about the binding site? Examination of the binding data in Table 1 [see also Gerzon *et al*. (1993),

K. E. Mitchell *et al*. (unpublished results), and Welch *et al*. (1994)] indicates that bulky substitutions at the 9- and 10-positions of ryanodine have little effect on binding. Therefore, the receptor places few, if any, steric constraints upon the ligand at that location. Consistent with that observation, introduction of charge also produces only minor changes in binding (about 800 cal/mol, Table 1, β-alanyl and guanidinopropionyl). This value is comparable to the small interaction energies (<1 kcal/mol) reported for aqueous-faced ionic bonds or salt links (Dao-pin *et al*., 1994).

Previously, we presented a working model of the ryanodine binding site (Welch *et al*., 1996). Part of the ryanoid molecule, centered around the 3-position, is buried within the binding site. This region of ryanodine makes major contributions to the binding energy. The pyrrole group (3-position) is more complementary to a low conductance conformation of the RyR, whereas the isopropyl group (2-position) is more complementary to a high conductance conformation. The rationale for this view can most easily be seen by examination of Figure 8 and by comparing the fractional conductances of ryanodine and ryanodol in Table 1. The net interaction of these two groups yields the conductance level detected in the electrophysiological experiments. Another part of the ryanoid, particularly the 9- and 10-positions, extends out of the binding pocket. This view is supported by the relatively small changes in binding affinity caused by large increases in steric bulk at this locus. Adducts at these positions are available for at least two types of interactions. The pendent groups may extend into the ion channel and directly retard the passage of cations. Alternatively, they may interact with other parts of the RyR structure inducing conformational changes in the RyR and block the ability of the protein to form the fully open channel. These possibilities are explored further below.

Relationship between the Ryanodine Binding Site and the Ca^{2+} Channel

The mechanism by which a functional, high-affinity binding site is created in the RyR remains unknown. Assembly of the tetrameric form of the RyR is apparently required. High-affinity binding is observed only in the tetrameric structure (Ogawa, 1994). It has been suggested that the tetramer contains one high-affinity (Lai *et al*., 1988a) and two to three low-affinity binding sites (Lai *et al*., 1989; McGraw *et al*., 1989; Pessah & Zimanyi, 1991). Callaway *et al*. (1994) using a combination of proteolysis and binding experiments implicate the region between Arg-4475 and the C terminus of the RyR as part of the ryanodine binding site. This locates the ryanodine binding site near or between the putative transmembrane regions. Photoaffinity labeling was used to locate the ryanodine binding site in the same 76 kDa C-terminal fragment (Witcher *et al*., 1994). However, the size of this fragment still leaves uncertainty in the spatial distance between bound ryanodine and the amino acid residues comprising the ion channel. A ryanoid may bind within the Ca^{2+} channel, or it may bind at a site remote from the channel. Wherever ryanodine binds, it produces two distinct alternations in RyR channel behavior. It both stabilizes open (or conducting) forms of the channel and alters the conductance of the open conformation. We have found correlations between ryanodine structure and two biological activities, high-affinity binding and fractional conductance. Can information from the CoMFA provide insights into the spatial relationship between the ion channel and the ryanodine binding site? The structure−function analysis of the ryanoid effects is far from complete; however, results to date are helpful.

For purposes of this discussion, we will consider the ryanodine effect in terms of two simple mechanisms. In one (a plug mechanism), the ryanoid is hypothesized to bind in the conduction pathway and directly interact with the permeant cation during transit through the RyR. In an elementary case, this might correspond to direct competitive inhibition where ryanoid and cation compete for an overlapping binding site. In the second model (an allosteric mechanism), ligand-induced conformational changes in the RyR mediate the interactions between the ryanoid and permeant cation. In this latter model, ryanodine corresponds to an allosteric modulator.

Plug Mechanism. This model requires that ryanodine directly occlude the conduction path. In principle, it is possible to test the hypothesis by examination of the relationship between additional steric bulk and electrostatic charge and the fractional conductance. To a first approximation, we can consider the 9- and 10-positions as extending into a foyer (Welch *et al*., 1996). Note that addition of bulky steric groups has little effect on the dissociation constant (Table 1). For purposes of analysis of the plug model, we consider the foyer to be part of the ion conduction path.

Effect of Steric Bulk on Fractional Conductance. The CoMFA can be used to separate the steric and electrostatic components modulating fractional conductance. Table 1 contains a quantitative analysis of all compounds tested. In one column, the predicted fractional conductances are listed. Note the close agreement between experiment and CoMFA. The adjacent column lists the fractional conductance predicted considering only steric interactions. The method used for this calculation is outlined in the legend of Table 1. Consider ryanodine as an example. The predicted fractional conductance is 58%. The steric bulk alone is calculated to produce a value for fractional conductance of 57%. In short, essentially all of the observed perturbation of conductance by ryanodine is due to steric effects. In contrast, consider guanidinopropionyl. The predicted fractional conduction is 8%; the estimate of fractional conductance arising from steric bulk alone is 48%. In this case, steric and electrostatic forces contribute about equally. In other words, although the molecular volume of guanidinopropionyl is considerably larger than that of ryanodine, steric forces contribute only half of the observed reduction in conductance. Comparisons for other ryanoids are shown in Table 1. According to the plug mechanism, at least part of the bound ryanoid blocks the transit of the permeant ion. The extreme distance dependency of repulsive steric interactions (r^{12}, Tinoco *et al*., 1995) makes steric occlusion of the channel highly detectable; changes will be either negligible or massive. Stated in other terms, should steric occlusion be a factor, small increases in size will produce large changes in the observed property (see the example of ryanodyl nicotinate below). Consequently, the graded response seen with this basis set is not expected. Two examples are used to illustrate the latter point. The observed fractional conductances induced by CBZ glycyl and 21-*p*-nitro are due almost entirely to the steric bulk of these ligands. The CBZ glycyl group extends the molecule an average of 7 Å (from molecular dynamics, data not shown) and increases the volume by 148

Å^3. The *p*-nitrobenzyl group extends ryanodine 7 Å and increases the volume 119 Å^3. These large, but electrically neutral, groups cause a relatively minor decrease in binding affinity [Table 1; see also Gerzon *et al*. (1993) and Welch *et al*. (1994)].

A comparison of structural differences between ryanodyl nicotinate (Welch *et al*., 1994) and ryanodine is used as an illustration of expected changes in a biological property if steric repulsion were important. Replacement of the pyrrole (ryanodine) by a pyridine (ryanodyl nicotinate) extends the molecule an average of 0.5 Å and increases the volume by 11 Å^3. The comparatively slight change in length and volume increased the dissociation constant 160-fold (3.1 kcal/mol), far greater than any of the effects on fractional conductance reported here. Because, as we have seen, increased steric bulk has far less effect on fractional conductance, it is unlikely that direct steric conflict between ryanoid and permeant cation is the mechanism of reduced fractional conductance.

Our observation that increased molecular volume has little effect on fractional conductance is consistent with those of Lindsay *et al*. (1994). These workers found that ryanodine binding increased conductance and permeability of large cations (diethylammonium ion) but had little effect on the permeability of small cations (K^+, ammonium). If direct steric interactions between ryanodine and permeant ion were important, large cations should have been inhibited more than small cations.

Effect of Electrostatic Charge. As in the case of increases in molecular size, the plug mechanism leads to certain expectations about the effect of electrostatic charge. One would expect a simple Coulomb's Law relationship (Voet & Voet, 1990). We can use this simple model of electrostatic interaction to estimate the distance between the ryanoid and the permeant ion. The guanidinopropionyl group extends the ryanoid molecule an average of 8 Å. The volume is increased 99 Å^3. In comparison, the β-alanyl derivative extends the molecule 3 Å and increases the volume 63.5 Å^3. Note, although the positive charge is located at different distances from the 10-position, there is no essential difference in the binding of these two ryanoids (Table 1). This fact again indicates there is no apparent restriction at this site [see also Welch *et al*. (1996)]. Using the CoMFA, we calculated that electrostatic forces contributing to the reduction in the fractional conductance are 1104 and 933 cal/mol for guanidinopropionyl and β-alanyl, respectively. The distance between these ryanoids and the permeant cation (in this case K^+) can be estimated using point charges and Coulomb's Law as mentioned above. We have used SYBYL, the molecular structures of the ryanoids and potassium ion, and explicit solvation by water to provide a better approximation of the electrostatic interaction. Preliminary calculations indicate that, for 1 kcal/mol of electrostatic energy, there is an 8 Å or greater distance between the charged atom on the ryanoid and potassium ion. For comparison with direct metal interactions, the distances between Ca^{2+} and the coordinating ligand atoms of several Ca^{2+} binding proteins range between 1.6 and 3.3 Å (Nayal & Di Cera, 1994, and references therein). These latter distances include proteins with Ca^{2+} affinities consistent with the estimated dissociation constant of Ca^{2+} from the channel of ryanodine receptor (Tinker *et al*., 1993; also see below). Therefore, both steric and electrostatic data indicate that there is a relatively large distance between ryanoid and permeant ion. Either the channel is quite large, or ryanodine binds outside of the channel.

In summary, the CoMFA leads to inconsistencies with the plug model. For example, if ryanodine binding is able to act directly to block K^+ transit, then ryanodine must bind in a confined area through which K^+ must pass. However, the relatively weak perturbation of both binding and fractional conductance by substituents at the 9- and 10-positions of ryanodine requires an open or unconstricted area. Such an area would likely be filled with water. However, if ryanodine binding occurs in a large vestibule, it is difficult to explain how the ligand could directly block K^+ transit. The circumstantial nature of these observations does allow one to rule out a plug mechanism. However, none provides support for the plug mechanism.

Allosteric Mechanism. In this mechanism, the binding of a ryanoid modulator can be at some distance from the cation conduction pathway. Both the electronic and steric properties of the ryanoid modulate cation conductance by inducing or stabilizing a low-conductance conformation of the RyR (Figures 3, 5, 8, and 9). Ryanodine is acting as a heterotropic, allosteric modulator. Ryanodine binding not only alters fractional conductance of the RyR but also induces a long-lived open form of the channel. An allosteric mechanism provides an explanation for the gating behavior. Allosteric modulators are thought to selectively stabilize one or more conformers of a protein that exists in a manifold of conformations. In an allosteric mechanism, the stabilization of a conductance state and the alteration of conductance are necessarily linked. The CoMFA provides no direct evidence for, but is consistent with, an allosteric mechanism. In contrast, the plug model has inconsistencies with the CoMFA as noted above.

In an allosteric model, binding energy is converted into conformational transitions in the protein. These conformational transitions selectively stabilize or destabilize intermediates and/or transition states in the conduction path model proposed by Tinker *et al*. (1992). Some modulators of RyR Ca^{2+} channel behavior are known to bind remotely from the transmembrane domain (Wagenknecht & Radermacher, 1995, and references therein). The ryanoids may act in a similar manner. Additional support for allosteric modulation comes from the studies of choline and glucose permeability through the RyR (Kasai & Kawasaki, 1993). These workers found that the Ca^{2+}-induced open form of the channel is modulated by KCl. For example, glucose will pass through the RyR only in the presence of high concentrations of KCl. Multiple open forms of the RyR are consistent with allosteric modulation.

How might ryanodine-mediated conformational changes modulate fractional conductance of the RyR *via* an allosteric mechanism? It has been noted (Nayal & Di Cera, 1994; Yamashita *et al*., 1990) that practically all Ca^{2+}-binding sites consist of concentric shells of hydrophilic (inner) and hydrophobic (outer) groups. Nayal and Di Cera (1994) point out the relationship between binding energy and ligation distance. Tinker *et al*. (1993) have estimated the dissociation constant of Ca^{2+} to the channel of the ryanodine receptor to be 100−200 μM. This is within the range of proteins considered by Nayal and Di Cera (1994). The ion conduction pathway may possess structural characteristics similar to those of Ca^{2+} binding proteins. Lindsay *et al*. (1994)

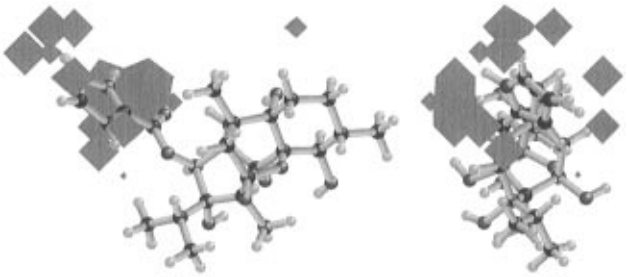

FIGURE 10: Orthogonal diagram illustrating the location of the major steric forces responsible for the tight binding of ryanodine to the RyR. A stick model of ryanodine is shown for orientation. The pyrrole is on the left of the left-hand drawing. The pyrrole is above the plane of the right-hand drawing. A contour plot of the ryanodine CoMFA field multiplied by the partial least-squares coefficients indicates the regions of the ryanodine molecule responsible for the observed dissociation constant. The contribution field is contoured at the 80% level.

envisioned negative charge throughout the conduction pathway. Conformational changes induced by ryanodine binding could produce alterations in the ligation distance between cation and protein, thus altering either the ground state energies of the intermediates or the energies of the transition states of the conduction pathway or both.

Comparison of Ryanoid Structure Modulating Fractional Conductance and Binding Energy. The interrelationships between ryanoid structure, binding energy, and the fractional conductance of the RyR are clues into RyR channel function. Briefly, the pyrrole locus (3-position) has the greatest influence on binding affinity, and adducts at the 10-position have relatively little effect (Table 1, CoMFA not shown; Welch *et al*., 1994, 1996; K. E. Mitchell *et al*., unpublished results). In addition, the pyrrole locus appears to be the chief factor determining the orientation of the bound ryanodine (Welch *et al*., 1996). For this paper, we have examined the correlation between the structure of the subset of ryanodine analogs listed in Table 1 and binding to cardiac SR. Figure 10 is contoured at 80% of the total contribution of the steric field to binding to illustrate the regions of the molecule that contribute most to the binding of ryanodine to the high-affinity site of cardiac SR. Note that most of the contribution is in the pyrrole region with an additional contribution near the 7- and 8-positions, consistent with previous analyses. The importance of the two positions is reversed when measuring fractional conductance; adducts at the 10-position have dramatic effects on fractional conductance, whereas contributions at the 3-position are of lesser importance.

Summary

Ryanodine binding modifies the articulation between RyR subunits required to generate a fully open channel. Modulation of cation conductance through the RyR is predominantly at the 10-position. A direct steric interaction between the bound ryanoid and the permeant cation is not supported by the data. The CoMFA suggests that the ryanodine binding site and the calcium channel are not coaxial as diagrammed by Wang *et al*. (1993). The relative importance of electrostatic and steric factors at the 10-position on fractional conductance compared to the relatively minor effects on binding suggests the possibility of engineering ligands capable of binding tightly to the RyR but producing quite different alterations in RyR channel function.

REFERENCES

Ashley, R. H., & Williams, A. J. (1990) *J. Gen. Physiol. 95*, 981−1005.

Bernstein, F. C., Koetzle, T. F., Williams, G. J. B., Meyer, E. F., Jr., Brice, M. D., Rodgers, J. R., Kennard, O., Shimanouchi, T., & Tasumi, M. (1977) *J. Mol. Biol. 112*, 535−542.

Brillantes, A.-M. B., Ondrias, K., Scott, A., Kobrinsky, E., Ondriasova, E., Moschella, M. C., Jayaraman, T., Landers, M., Ehrlich, B. E., & Marks, A. R. (1994) *Cell 77*, 513−523.

Brown, I. D., & Wu, K. K. (1976) *Acta Crystograllogr. B32*, 1957−1959.

Callaway, C., Seryshev, A., Wang, J.-P., Slavik, K. J., Needleman, D. H., Cantu, C., III, Wu, Y., Jayaraman, T., Marks, A. R., & Hamilton, S. L. (1994) *J. Biol. Chem. 269*, 15876−15884.

Campbell, K. P., Franzini-Armstrong, C., & Shamoo, A. E. (1980) *Biochim. Biophys. Acta 602*, 97−116.

Campbell, K. P., Knudson, C. M., Imagawa, T., Leung, A. T., Sutko, J. L., Kahl, S. D., Raab, C. R., & Madson, L. (1987) *J. Biol. Chem. 262*, 6460−6463.

Cho, S. J., & Tropsha, A. (1995) *J. Med. Chem. 38*, 1060−1066.

Clark, M., Cramer, R. D., III, & Van Opdenbosch, N. (1989) *J. Comput. Chem. 10*, 982−1012.

Coronado, R., Morrissette, J., Sukhareva, M., & Vaughan, D. M. (1994) *Am. J. Physiol. 266*, C1485−C1504.

Cramer, R. D., III, Patterson, D. E., & Bunce, J. D. (1988) *J. Am. Chem. Soc. 110*, 5959−5967.

Dao-pin, S., Sauer, U., Nicholson, H., & Matthews, B. W. (1991) *Biochemistry 30*, 7142−7153.

Deslongchamps, P., Bélanger, A., Berney, D. J. F., Borschberg, H.-J., Brousseau, R., Doutheau, A., Durand, R., Katayama, H., Lapalme, R., Leturc, D. M., Liao, C.-C., MacLachlan, F. N., Maffrand, J.-P., Marazza, F., Martino, R., Moreau, C., Ruest, L., St-Laurent, L., Saintonge, R., & Soucy, P. (1990) *Can. J. Chem. 68*, 115−192.

Ellisman, M. H., Deerinck, T. J., Ouyang, Y., Beck, C. F., Tanksley, S. J., Walton, P. D., Airey, J. A., & Sutko, J. L. (1990) *Neuron 5*, 135−146.

Fleischer, S., & Inui, M. (1989) *Annu. Rev. Biophys. Biophys. Chem. 18*, 333−364.

Fruen, B. R., Mickelson, J. R., Shomer, N. H., Velez, P., & Louis, C. F. (1994) *FEBS Lett. 352*, 123−126.

Gerzon, K., Humerickhouse, R. A., Besch, H. R., Jr., Bidasee, K. R., Emmick, J. T., Roeske, R. W., Tian, Z., Ruest, L., & Sutko, J. L. (1993) *J. Med. Chem. 36*, 1319−1323.

Giannini, G., Clementi, E., Ceci, R., Marziali, G., & Sorrentino, V. (1992) *Science 257*, 91−94.

Giannini, G., Conti, A., Mammarella, S., Scrobogna, M., & Sorrentino, V. (1995) *J. Cell Biol. 128*, 893−904.

Green, S. M., & Marshall, G. R. (1995) *Trends Pharmacol. Sci. 16*, 285−291.

Hawkes, M. J., Nelson, T. E., & Hamilton, S. L. (1992) *J. Biol. Chem. 267*, 6702−6709.

Hille, B. (1992) *Ionic Channels of Excitable Membranes*, 2nd ed., Sinauer Associates, Inc., Sunderland, MA.

Humerickhouse, R. A., Besch, H. R., Jr., Gerzon, K., Ruest, L., Sutko, J. L., & Emmick, J. T. (1993) *Mol. Pharmacol. 44*, 412−421.

Humerickhouse, R. A., Bidasee, K. R., Gerzon, K., Emmick, J. T., Kwon, S., Sutko, J. L., Ruest, L., & Besch, H. R., Jr. (1994) *J. Biol. Chem. 269*, 30243−30253.

Inui, M., Saito, A., & Fleischer, S. (1987) *J. Biol. Chem. 262*, 1740−1747.

Jefferies, P. R., Lam, W.-W., Toia, R. F., & Casida, J. E. (1992) *J. Agric. Food Chem. 40*, 509−512.

Jenden, D. J., & Fairhurst, A. S. (1969) *Pharmacol. Rev. 21*, 1−25.

Kasai, M., & Kawasaki, T. (1993) *J. Biochem. 113*, 327−333.

Lai, F. A., Erickson, H. P., Rousseau, E., Liu, Q.-Y., & Meissner, G. (1988a) *Nature 331*, 315−319.

Lai, F. A., Anderson, K., Rousseau, E., Liu, Q.-Y., & Meissner, G. (1988b) *Biochem. Biophys. Res. Commun. 151*, 441−449.

Lai, F. A., Misra, M., Xu, L., Smith, H. A., & Meissner, G. (1989) *J. Biol. Chem. 264*, 16776−16785.

Ledbetter, M. W., Preiner, J. K., Louis, C. F., & Mickelson, J. R. (1994) *J. Biol. Chem. 269*, 31544−31551.

Lindsay, A. R. G., & Williams, A. J. (1991) *Biochim. Biophys. Acta 1064*, 89−102.
Lindsay, A. R. G., Tinker, A., & Williams, A. J. (1994) *J. Gen. Physiol. 104*, 425−447.
Marks, A. R., Tempst, P., Hwang, K. S., Taubman, M. B., Inui, M., Chadwick, C., Fleischer, S., & Nadal-Ginard, B. (1989) *Proc. Natl. Acad. Sci. U.S.A. 86*, 8683−8687.
McGrew, S. G., Wolleben, C., Siegl, P., Inui, M., & Fleischer, S. (1989) *Biochemistry 28*, 1686−1691.
McPherson, P. S., & Campbell, K. P. (1993) *J. Biol. Chem. 268*, 13765−13768.
Meissner, G. (1975) *Biochim. Biophys. Acta 389*, 51−68.
Meissner, G. (1994) *Annu. Rev. Physiol. 56*, 485−508.
Meissner, G., & El-Hashem, A. (1992) *Mol. Cell. Biochem. 114*, 119−123.
Nayal, M., & Di Cera, E. (1994) *Proc. Natl. Acad. Sci. U.S.A. 91*, 817−821.
Ogawa, Y. (1994) *Crit. Rev. Biochem. Mol. Biol. 29*, 229−274.
Padua, R. A., Nagy, J. I., & Geiger, J. D. (1996) *Eur. J. Pharmacol. 298*, 185−189.
Pessah, I. N., & Zimanyi, I. (1991) *Mol. Pharmacol. 39*, 679−689.
Pessah, I. N., Francini, A. O., Scales, D. J., Waterhouse, A. L., & Casida, J. E. (1986) *J. Biol. Chem. 261*, 8643−8648.
Rogers, E. F., Koniuszy, F. R., Shavel, J., Jr. & Folkers, K. (1948) *J. Am. Chem. Soc. 70*, 3086−3088.
Rousseau, E., Smith, J. S., & Meissner, G. (1987) *Am. J. Physiol. 253*, C364−C368.
Ruest, L., & Deslongchamps, P. (1993) *Can. J. Chem. 71*, 634−638.
Ruest, L., Taylor, D. R., & Deslongchamps, P. (1985) *Can. J. Chem. 63*, 2840−2843.
Shoshan-Barmatz, V., Pressley, T. A., Higham, S., & Kraus-Friedmann, N. (1991) *Biochem. J. 276*, 41−46.
Sutko, J. L., & Willerson, J. T. (1980) *Circ. Res. 46*, 332−343.
Sutko, J. L., & Airey, J. A. (1996) *Physiol. Rev. 76*, 1027−1071.
Sutko, J. L., Willerson, J. T., Templeton, G. H., Jones, L. R., & Besch, H. R., Jr. (1979) *J. Pharmacol. Exp. Ther. 209*, 37−47.
Sutko, J. L., Thompson, L. J., Schlatterer, R. G., Lattanzio, F. A., Fairhurst, A. S., Campbell, C., Martin, S. F., Deslongchamps, P., Ruest, L., & Taylor, D. R. (1986) *J. Labelled Compd. Radiopharm. 23*, 215−222.
Takeshima, H., Nishimura, S., Matsumoto, T., Ishida, H., Kangawa, K., Minamino, N., Matsuo, H., Ueda, M., Hanaoka, M., Hirose, T., & Numa, S. (1989) *Nature 339*, 439−445.
Tinker, A., Lindsay, A. R. G., & Williams, A. J. (1992) *J. Gen. Physiol. 100*, 495−517.
Tinker, A., Lindsay, A. R. G., & Williams, A. J. (1993) *Cardiovasc. Res. 27*, 1820−1825.
Tinker, A., Sutko, J. L., Ruest, L., Deslongchamps, P., Welch, W., Airey, J. A., Gerzon, K., Bidasee, K. R., Besch H. R., Jr., & Williams, A. J. (1996) *Biophys. J. 70*, 2110−2119.
Tinoco I., Jr., Sauer, K., & Wang, J. C. (1995) *Physical Chemistry*, p 472, Prentice Hall, Upper Saddle River, NJ.
Voet, D., & Voet, J. G. (1990) *Biochemistry*, p 175, Wiley, New York.
Wagenknecht, T., & Radermacher, M. (1995) *FEBS Lett. 369*, 43−46.
Wang, J. P., Needleman, D. H., & Hamilton, S. L. (1993) *J. Biol. Chem. 268*, 20974−20982.
Waterhouse, A. L., Pessah, I. N., Francini, A. O., & Casida, J. E. (1987) *J. Med. Chem. 30*, 710−716.
Welch, W., Ahmad, S., Airey, J. A., Gerzon, K., Humerickhouse, R. A., Besch H. R., Jr., Ruest, L., Deslongchamps, P., & Sutko, J. L. (1994) *Biochemistry 33*, 6074−6085.
Welch, W., Sutko, J. L., Mitchell, K. E., Airey, J., & Ruest, L. (1996) *Biochemistry 35*, 7165−7173.
Wiesner, K. (1972) *Adv. Org. Chem. 8*, 295−316.
Witcher, D. R., McPherson, P. S., Kahl, S. D., Lewis, T., Bently, P., Mullinnix, M. J., Windass, J. D., & Campbell, K. P. (1994) *J. Biol. Chem. 269*, 13076−13079.
Yamashita, M. M., Wesson, L., Eisenman, G., & Eisenberg, D. (1990) *Proc. Natl. Acad. Sci. U.S.A. 87*, 5648−5652.
Zaidi, M., Shankar, V. S., Alam, A. S. M. T., Moonga, B. S., Pazianas, M., & Huang, C. L.-H. (1992) *Biochem. Biophys. Res. Commun. 188*, 1332−1336.
Zucchi, R., Ronca-Testoni, S., Yu, G., Galbani, P., Ronca, G., & Mariani, M. (1995) *Br. J. Pharmacol. 114*, 85−92.

BI9623901